This is the preprint of : in IEEE Transactions on Plasma Science, vol. 45, no. 1, pp. 113-120, Jan. 2017, doi: 10.1109/TPS.2016.2633400

Electric Arc in Low Voltage Circuit Breakers: Experiments and Simulation

A Iturregi, B Barbu, E Torres, F Berger and I Zamora, *Member, IEEE*

***Abstract*—The aim of this paper is to present a further approach for analyzing the air electric arc in Low Voltage Circuit Breakers (LVCBs). In order to achieve that, a new simulation model and experimental tests have been carried out. The simulation model has been designed using ANSYS CFX, a Finite Volume Method (FVM) commercial software. This model has been defined as a 3D geometry, with a high density structured hexaedral mesh, P1 radiation model and hot air characteristics for thermal plasma properties and transport coefficients. The model is applied to simulate the behavior of a LVCB for 50A, 100A and 200A with different number of splitter plates in the arc chamber and different locations for the arc ignition. As result, arc elongation and arc voltage increase have been observed when increasing the splitter plates number. Also faster arcs for higher ignition zones and greater expansion and diffusion for higher input currents have been obtained. These simulation results have been verified and validated. The verification process has been accomplished calculating the numerical errors, by means of the Grid Convergence Index (GCI) and Courant-Friedrichs-Lewis (CFL) number. Thus, the most accurate mesh densities, time steps and radiation models have been selected. Finally, the validation process has been achieved performing real experimental tests in the laboratory, proving that the results of the simulation model are close to real scenarios.**

***Index Terms*—Circuit Breakers, Arc discharges, Simulation, Finite volume methods, Laboratories.**

I. Introduction

ELECTRIC arc phenomenon is an important topic in different research communities due to its wide application in major industrial fields and its physical complexity [1]. In circuit breakers, an electric arc is formed at the contact separation time. In order to create a reliable switch off process a good knowledge regarding the arc formation, development and interaction with the surrounding parts is mandatory.

There are two main approaches for the research and development of a switching device: experiments and simulation. Experimental research provides real properties of the arc discharge. As a drawback, the data obtained is usually spatially or temporally limited. On the other hand, simulation provides a better spatial and temporal visualization of the computed physical arc characteristics, avoiding the need of building and testing numerous and costly prototypes. The main drawback of simulation modeling is the high complexity of the discharge physics that cannot always be reproduced accurately by a mathematical system. In any case, once the simulation model has been designed verification and validation processes must be carried out in order to prove its validity.

The most accurate simulation modeling of the electric arc is nowadays obtained through magnetohydrodynamic (MHD) physical models. In these models, a coupled set of equations is used to describe the plasma behavior. The modified Navier-Stokes set of partial differential equations (PDE) representing the conservation of mass, momentum and energy are used to describe the plasma flow. The interaction with the electromagnetic field is done by coupling and solving at the same time the well-known Maxwell equations.

Industrial and academic institutions have lead the research and development of those electric arc computational models. At TU Braunschweig, Lindmayer et al. focused their efforts on parallel or divergent rails geometrical models with one or more splitter plates, analyzing the effect of the arc roots [2-10]. All the models are developed as 3D geometries with quarter symmetry in order to reduce the computational time. The different radiation models used are based either on a simplified form of the Boltzman equation or the Net Emission Coefficient (NEC) method. The arc flow movement, the arc voltage, pressure or temperature values are analyzed and validated against experimental data. However, the settings for the arc root model and radiation model should be improved, as their simplicity can lead to inaccurate flow results.

In the models presented by Li et al. from Xi'an Jiaotong University [11-15] the effect of several influence factors has been analyzed. Their studies are performed using variations of: the arc ignition position, the compositions used as interruption medium, the venting size or the splitter plates shape. In these simulations, the radiation model is more accurate (e.g. P1 approximation) but the geometries are simplified consisting on a 2D half symmetry model with simplified electrodes and no rails. An improvement to the above-mentioned models is presented in [16]. Based on previous works from Lindmayer et al., this simulation model implements a simplified arc roots description. This model presents interesting advances although an unrealistic symmetry condition is considered in the arc flow and the radiation model should be improved.

Finally, several models are presented by the manufacturing companies such as Siemens [1, 17] or Schneider Electric [18,

This work was supported in part by the UPV/EHU under project EHU09/45.

A. Iturregi, E. Torres and I. Zamora are with Department of Electrical Engineering, University of the Basque Country (UPV/EHU), Bilbao, 48013, Spain (e-mail: araitz.iturregi@ehu.es, esther.torresi@ehu.es, inmaculada.zamora@ehu.es)

B. Barbu and F. Berger are with Department of Electrical Apparatus and Switchgears, Technical University of Ilmenau, Ilmenau, 98693, Germany (e-mail: bogdan.barbu@tu-ilmenau.de, frank.berger@tu-ilmenau.de)

19]. In these models, geometries are quite complex and closer to real scenarios, but little public information is available.

In this paper, a new electric arc simulation model for a LVCB and its verification process are described in section II. In section III the results obtained for different cases are shown and section IV presents the experimental results that validates the model. Finally, in section V the conclusions are summarized.

II. New Electric Arc Modeling for LVCB

In this section, the characteristics of the new simulation model are fully described. The improvements included in the model, the meshing parameters as well as boundary and initialization conditions are explained in subsection II-A. After that, in subsection II-B, the verification process to quantify and minimize the numerical errors appearing in these type of simulations is presented.

A. Description of the Proposed Model

The proposed model for the analysis of the air electric arc has been built taking as reference the model presented in [16]. As presented in Fig. 1b), this model represents a simplification of the LVCB geometry being composed of an anode, cathode and a splitter plate system. The simulation model has been designed using the commercial software Ansys CFX. The dimensions have been maintained as in the reference model, so that a comparison of results can be made. However, several improvements have been included in the new model proposed, comparing to the reference model:

1) A full 3D geometry, without any computational symmetry condition has been designed (Fig. 1b)) ;
2) A high density structured hexahedral mesh of approximately 1,000,000 elements has been defined;
3) New thermal plasma properties and transport coefficients are implemented according to [20];
4) An improved radiation model, P1, has been defined, after comparing Net Emission Coefficient (NEC), Simplified Net Emission Coefficient (NECS) and P1 models in the verification process [21];
5) Magnetic vector potential calculation is adopted for computing the magnetic field distribution.

The mesh of the model has been built using the software tool ICEM CFD in order to obtain a better accuracy of the cells distribution. A structured hexahedral mesh is chosen for the entire model. Finer mesh elements are defined at the fluid-solid interfaces and at the fluid edges due to the high gradients in the flow field variables. The mesh characteristics are presented in Table I. A first step performed in order to check the mesh accuracy has been to compare the maximum and minimun values obtained for certain mesh parameters (i.e. aspect ratio, volume change, minimum angle, mesh determinant) with the reference values provided by ICEM CFD. As shown in Table II all the parameter values are validated with success. Besides, in order to asses the quality of the used computational mesh a further analysis is presented in subsection II-B.

The solid parts of the model consisting of the cathode, the anode and splitter plates have been defined as copper, while

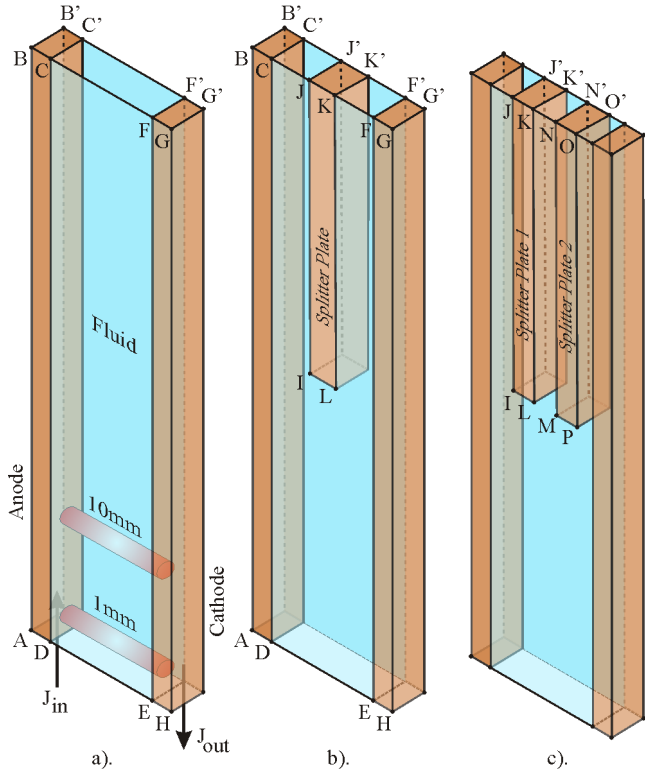

Fig. 1. Geometry designed for the LVCB arc chamber for a) zero splitter plate (0SP), b) one splitter plate (1SP) and c) two spliter plates (2SP)

TABLE I
Description of the Mesh

Edge Name	Edge length [mm]	Nodes number	Total elements	Total nodes
BB'	2.5	25	1,144,546	1,057,350
BC	1.55	15		
CJ	3.0	30		
JK	2.0	20		
KF	3.0	30		
FG	1.5	15		
HI	20.0	200		
HG	40.0	400		

the fluid part as air with variable properties as a function of temperature.

The boundary conditions are defined based on the reference model [16] and are presented in Table III. At the boundaries between the model and the regions outside (i.e. at the front and back walls of the air, splitter plate, electrodes and the lower part of the air) no thermal exchange is considered (e.g. adiabatic boundary condition). No external magnetic fields are applied as well. The solid walls have been defined by a non slippery condition (i.e. fluid velocity is zero at the walls in contact with the fluid). At the interfaces between air-electrodes and air-splitter plate system, the temperature exchange has been also defined as adiabatic. Regarding electric and magnetic fields, Conservative Interface Flux (CIF) is applied at the interfaces. It implies that variables will flow between both sides of the interface. Once again, the wall is defined with a non-slippery boundary condition. At the top face, the opening of the air volume is

TABLE II
MESH QUALITY

Parameter	Reference Value		Obtained Value	
	Min	Max	Min	Max
Aspect ratio	1	1000	1	2.98
Volume change	1	20	1	1.69
Angle	25°	-	90°	90°
Determinant	0.2	-	1	1

TABLE III
BOUNDARY CONDITIONS USED IN THE SIMULATION MODEL

Boundary	T(K)	p_{abs} (atm)	Electric field	Magnetic field	Boundary type
Outer interfaces: ABGH/A'B'G'H' DD'EE'/BB'CC' JJ'KK'/FF'GG'	Adiab.	-	Zero flux	Zero flux	No slip wall
Solid-Fluid interfaces: CC'DD'/JJ'II' II'LL'/KK'LL' FF'EE'	Adiab.	-	CIF	CIF	No slip wall
Openings: CC'JJ'/KK'FF'	300	1	Zero flux	A_i=0(Tm)	Opening
Anode down: AA'DD'	300	-	Flux In I=50(A)	Zero flux	Wall
Cathode down: EE'HH'	300	-	U=0(V)	Zero flux	Wall

at atmospheric conditions, thus temperature is set to 300K and the absolute pressure is 1atm. For the magnetic field, here the magnetic vector potential is set to 0.

Additionally, some other changes have been made regarding the reference model [16]. Temperature at the lower faces of anode and cathode has been changed from 300K to 500K, in order to improve the stability and avoid divergence errors due to the high difference of temperatures imposed at the initialization stage on the solid part and air volume. Regarding the magnetic field, in order to improve the reference model where an external magnetic field with a constant value of 0.1T is considered, in the model presented the magnetic field is calculated by Maxwell equations for each time step.

For the radiation modelling NECS, NEC and P1 have been tested in the new model. P1 radiation model is physically the most complete one, where absorption and emission coefficients are taken into account and the complete radiative spectrum is divided in several bands. In the NEC method, the real absorption coefficients are neglected and replaced by the net emission coefficients computed for an isothermal sphere and representing the difference between the energy emitted in the centre of the sphere and the energy emitted by all the other points of the sphere and absorbed by the central point. And finally, as the most simple model NECS method is found, where a linearization of the NEC is modeled. Each radiation model has been built with different references as base data: [16] for NECS, [22-24] for NEC and [21, 25] for P1. As it is demonstrated in the verification process, the best and most realistic option between the tested radiation models is P1 approximation. This model has been implemented using a six band subdivision of the arc radiation spectrum. Within each of these frequency bands, the spectral absorption coefficients of the plasma are set as a function of temperature. Therefore, for the implemented radiation model, the solver solves six extra differential equations in order to describe the energy transport in each band. This fact leads undoubtedly to an increased computational time, but the precision of the results is higher.

Regarding the arc roots phenomena, the local nonlinear resistance is implemented by the Additional Resistance option available in CFX for interfaces. The value for this nonlinear resistance is built according to a specific voltage-current density characteristic shown in Fig. 2. This characteristic shows that before a new arc root is formed, a certain ignition voltage has to be exceeded. Different values of ignition voltage are compared: 22.3V, 19.7V, 17.1V and 10V peaks obtaining similar simulation results for the four cases. This can be explained observing the current density values obtained in the simulations, which are much higher than the ones in the different voltage peaks. These voltage drop-current density values shown in Fig. 2 have been obtained from experimental results [5, 9] and describe in a macroscopic manner the entire series of physical processes taking place in the thin regions situated in the front of the electrodes.

The arc has been initialized as a hot cylindrical channel of 10,000K between the rails as shown in Fig. 1a). The total time of the simulation series has been set to 1ms and the time step 2.5μs. Results of the computed arc movement inside the experimental chamber with one splitter plate are presented for exemplification in Fig. 3. There, the arc movement behavior is represented by temperature isotherm in grey scale and current density in color vectors. It is illustrated how the arc moves upwards along the rails until it reaches the splitter plate, where it starts to bend and split until the total splitting of the arc.

B. Verification

In all the steps involved in a CFD analysis a certain amount of uncertainties and errors can arise depending on the complexity of the model [26, 27]. One of the possible sources of errors in the process of computing a certain

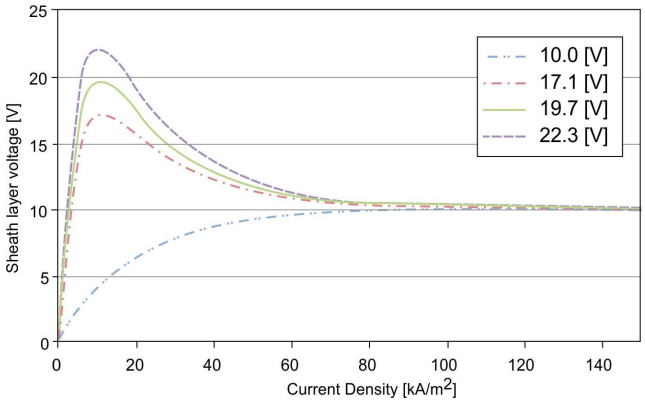

Fig. 2. Voltage drop-current density curve for new arc roots

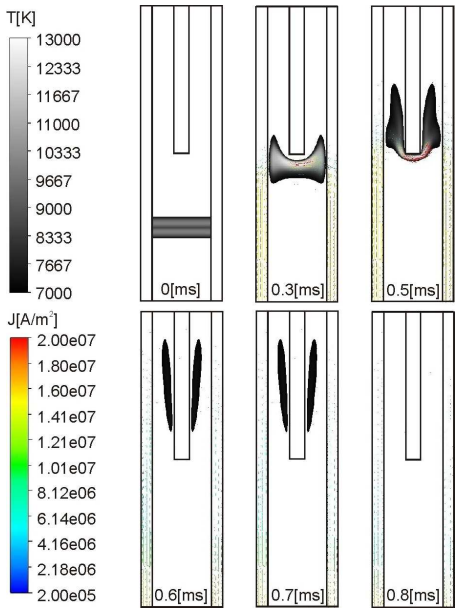

Fig. 3. Arc movement behavior obtained for the new arc model in LVCBs

TABLE IV
TOTAL NUMBER OF ELEMENTS OF EACH MESH

Mesh	Low Density	Medium Density	High density
Elements	572,273	1,144,546	1,716,819

simulation model is given by the chosen spatial and temporal discretization. Thereby, in order to perform the verification of the presented computational model, a systematically refinement of the grid size and the time step is necessary to evaluate its influence in the results obtained. In order to provide a consistent way for reporting the results from discretization studies, the Grid Convergence Index (GCI) [28, 29] and the Courant-Friedrichs-Lewis (CFL) number, reported directly by the CFX solver [29, 30], are proposed.

The aim of this verification process has been to select the most appropriate mesh size and time step for the model and to evaluate the results obtained for the three mentioned radiation models (NECS, NEC and P1), selecting the most stable and realistic approach. For that aim, different simulations have been performed on the proposed model. Regarding the mesh size, three different meshes have been analyzed according to Table IV. For the time step selection, three different time steps have been considered for the analysis: 1.25μs, 2.5μs and 5μs.

The additional settings needed for the solver, such as: total simulation time, transient time scheme (i.e. Second Order Backward Euler), inner iteration numbers for each time step and convergence criterion (i.e. Residual Target smaller than $1x10^{-4}$) are maintained constant. From the results of the tests performed on the proposed model [26, 27], it is concluded that the model presented in this work should be defined with a medium density mesh of around 1,000,000 elements and a time step of 2.5μs. Therefore, the smallest discretization errors and most stable and precise solutions on the arc behavior simulations are obtained.

III. RESULTS

Considering the improvements mentioned in the previous section of the paper, the model built has been used in order to analyze the effect of the splitter plates number and arc ignition position in the switching process.

A. Effect of the Splitter Plates

The effect of increasing the number of splitter plates has been analyzed by means of modified geometries as shown in Fig. 1, stating that increasing the number of splitter plates the arc voltage is increased.

A mathematical description of the arc voltage distribution is given by: $U_{arc} = U_c + E_c * l_c + U_a$ where U_c and U_a represent the cathode and anode voltage drop while E_c and l_c the arc column electric field and length.

As presented in Fig. 4, the main voltage increase for the model with 0SP, up to approximately 34V, is created in the first 0.1ms due to the expansion of the imposed hot conducting gas channel. This expansion results in an arc surface increase leading to higher energy losses with a resulting increase of the arc electric field strength E_c. After this point, when an energy balance is reached, the arc moves towards the upper side of the simulation chamber with a constant velocity and presenting a compact form (Fig. 5) but without any change on the voltage characteristic.

In the 1SP and 2SP models a similar behaviour as in the 0SP model can be observed up to 0.3ms, when the electric arc reaches the lower side of the splitter plate system. From this point on, the arc is bent around the splitter plate system, up to approximately 0.5ms, and then successfully splitted in partial arcs shortly before 0.6ms, as exemplary presented in Fig. 5 for the 2SP model. The bending phase results in an increase of the arc length l_c while the following split process creates additional cathode (U_c) and anode (U_a) voltage drops for each partial arc. This results, as presented in Fig. 4, in a voltage increase up to approximately 85V.

B. Arc Ignition Location and Input Current Values

In this test case, the arc ignition location has been changed from 10mm to only 1mm above the lower side of the computational model, as presented in Fig. 1. This change

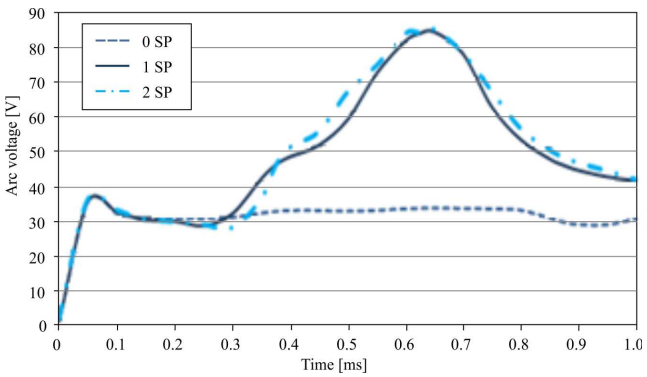

Fig. 4. Arc voltage for 0SP, 1SP and 2SP

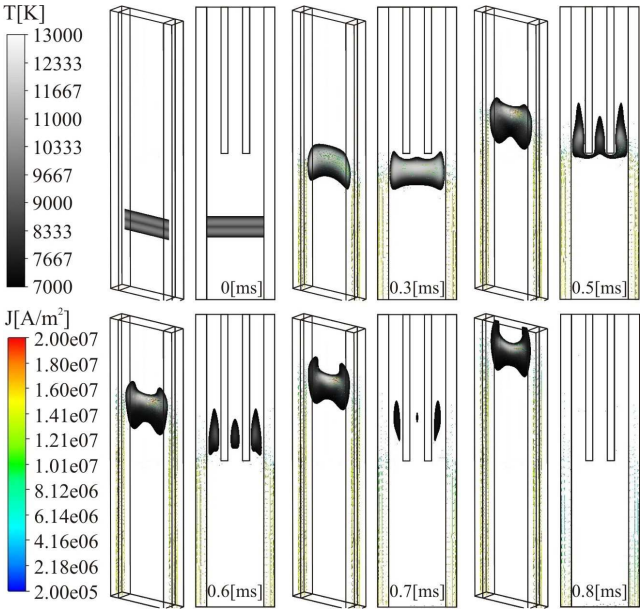

Fig. 5. Arc behavior for a model with 0SP and 2SP

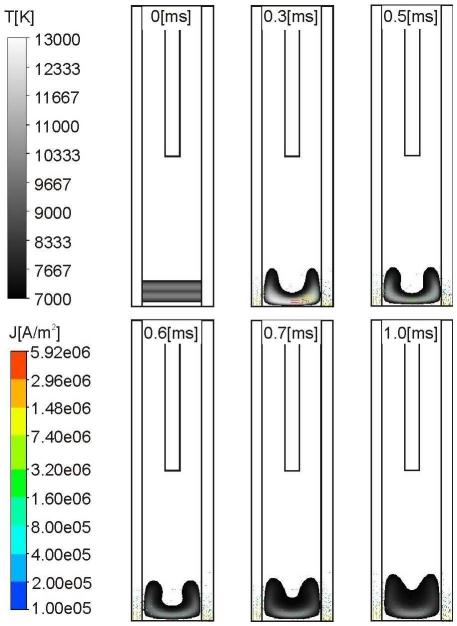

Fig. 6. Arc movement behavior for 50A and low ignition

has been applied for three different input currents (i.e. 50A, 100A and 200A) considering the 0SP and 1SP models. In all cases the total simulation time has been kept constant (i.e. 1ms). Comparing the results obtained for an 50A arc ignited at the lower position (Fig. 6) with a similar arc placed at the upper ignition point (Fig. 3), it can be observed that the arc in the first case barely moves upwards from the lower part of the arc chamber even after the total simulation time is reached.

An explanation for this behavior is given by the analysis of the flow development in the lower region of the simulation model. It can be observed that during the arc expansion period, the air in the region below the arc is pushed toward the lower inlet (i.e. surface DD'E'E in Table III). The reflected pressurized air constricts and pushes the arc toward one of the lateral walls creating a vortice region in front of the arc, with the flow velocity vectors pointing downward toward the arc column. The low electromagnetic forces (e.g Lorentz force) acting on the arc column are insufficient to counteract the fluid-dynamic forces and impose a forward movement. This behavior results in a temporary immobility of the arc in the lower part of the chamber.

In order to analyze the influence of the input current peak in the arc movement, 100A and 200A arcs have been simulated. In this current range, the high electromagnetic forces generated by the currents acts stronger on the arc column imposing an arc movement toward the upper outlet or the splitter plate system, as presented in Fig. 7 for a 200A arc. The same effect has been observed for a 100A arc in [31].

According to the presented results it can be concluded, in accordance with [12], that for lower arc currents a low arc ignition position leads to slower arc movements. These results are also sustained by the experimental tests developed and presented in the validation of the simulation model.

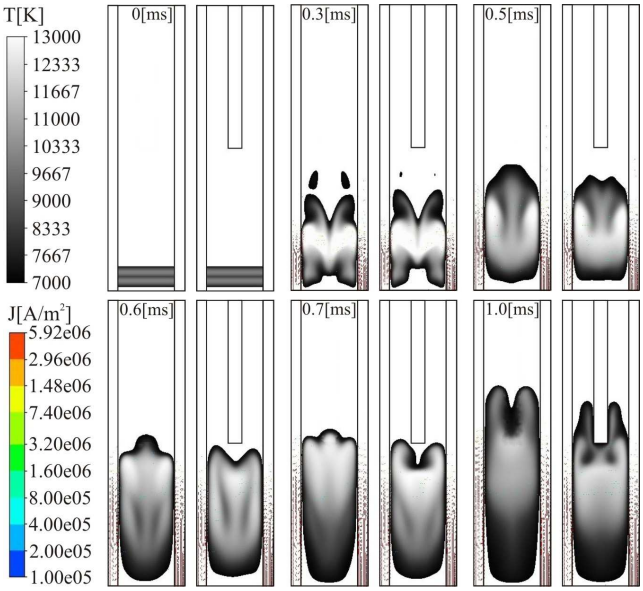

Fig. 7. Arc movement behavior for 200A and low ignition, 0SP in the left and 1SP in the right

IV. Validation

As a final step to prove the validity of the new air arc model for LVCBs, a set of experimental tests has been developed. In particular, a total of six different tests have been carried out, with three different input current values (50A, 100A and 200A) and two different geometries (arc chamber without splitter plate (0SP) and with one splitter plate (1SP)). In all the tests, the arc has been ignited at 1mm above the lower wall of the simulation model (low ignition), as shown in subsection III-B.

The experimental setup used for the laboratory tests is presented in Fig. 8. An impulse generator, which provides an impulse waveform 10/350, with a maximum charging voltage

of 10kV DC, has been used to provide the arc current. The generator is discharged over the series connection of the inductance and a variable resistance, at a given time specified by the Time Controller. Depending on the charging voltage and the value chosen for the variable resistor, different amplitudes of currents can be generated and applied in the experimental circuit. The inductance is used in order to damp the generated current so that an almost constant DC current form is obtained through the experimental time. The waveform of the generated current can be seen in Fig. 9 for all the current used in the experimental program. The geometric dimensions of the arcing chamber are the same as presented in Fig. 1.

Near the chamber, in order to record the evolution of the arc and the electrical magnitudes during the test, the following measurement equipment has been added to the circuit:

1) Two high-speed cameras. Hot Shot high speed video camera and HSFC Pro high speed photo camera, located in the right side of the scheme and focusing directly to the arc chamber.
2) A Pearson probe with a division rate of 1:1000 in order to measure the input current;
3) A Tektronix probe P1065A with division rate 1:1000, connected in parallel with the arc chamber to measure the arc voltage;
4) Two pressure PCB Piezoelectrics sensors with a division rate of 734 mV/bar located at 15 and 28mm above lower inlet, named P2 and P3 respectively;
5) Two LeCroy oscilloscopes with a maximum recording rate of 5GS/s used in order to record: the arc voltage, arc current and the pressure sensors data.

The high-speed cameras have been synchronized by a signal generated from an oscilloscope (Fig. 8). The video camera has an exposure time of 50μs while the photo camera has been used with exposure times of few ns (depending on the experiment current) but it only allows to take four pictures by experiment. Thus, the images from the video camera have been used to validate the arc displacement. Due to the higher exposure time of the video camera comparing to the simulations time step, the video camera images present an integration effect. The arc shape in this case is wider and the recorded luminosity is higher. In

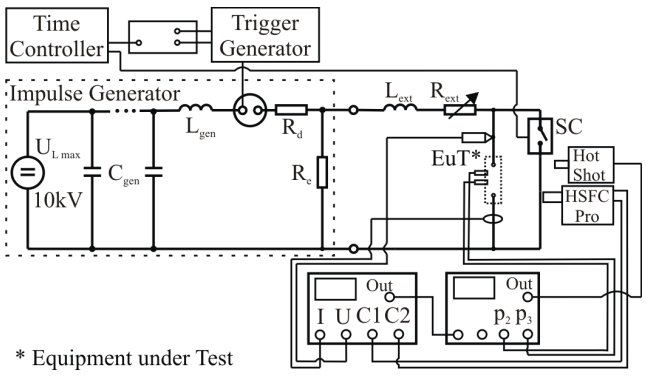

Fig. 8. Scheme of the electrical circuit and measurement system used in the laboratory tests

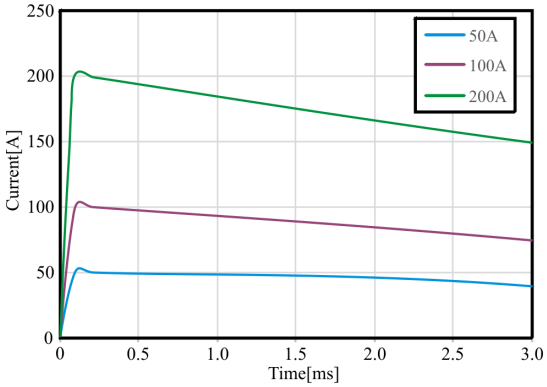

Fig. 9. Generated impulse current for the laboratory experiments

order to diminish the amount of light reaching the sensor of the video camera, the shutter has been set to the minimum allowed position. Apart from that, no other filters have been used for these experiments.

The arc movement recorded by the high speed video camera in the experiment for 50A and 0SP, is presented exemplary beside the simulation results in Fig. 10. By comparing the two image sets, a good qualitative agreement is observed. In both cases the arc burns in the lower part of the experimental setup during the first millisecond (i.e. the entire simulation time). It must be mentioned at this point that due to the ignition method used in the experiment, for the lower current range, the ignition electrode had to be positioned close to the cathode. This leads in some cases to an arc reignition in the lower area of the experimental chamber. Even so, it can be stated, by considering the fact that more experiments were completed during the experimental program, that this behaviour is characteristic for this experimental setup and this current range. An arc movement was observed in this case only when using long arcing time (i.e. in the range of 10ms) after at least 6ms and for distances smaller than 10mm.

The results for 200A, considering 0SP and 1SP, are shown in Fig. 11 and Fig. 12. A good correspondence with the results obtained in the simulations can be observed. The experiments show a strong arc expansion as the current increases and a much faster movement toward the upper edge of the experimental chamber with or without a splitter plate. This visual comparison with the simulation results is only from the phenomenological point of view since both plotted images can be influenced by different factors like the chosen exposure time, for the experiments, or the chosen temperature isotherm, in case of the simulation results. But nonetheless a correspondence between the two data sets with a good agreement can be observed.

Finally, a further validation can be carried out comparing the two data sets obtained in laboratory and simulations, for the maximum peak values of the pressure at P2 and P3 points. Thus, for instance, in 100A 0SP model, at P2 an overpressure of 0.176bar in experiments and 0.135bar in simulations have been obtained, while at P3 0.122bar in experiments and 0.14bar in simulations have been obtained.

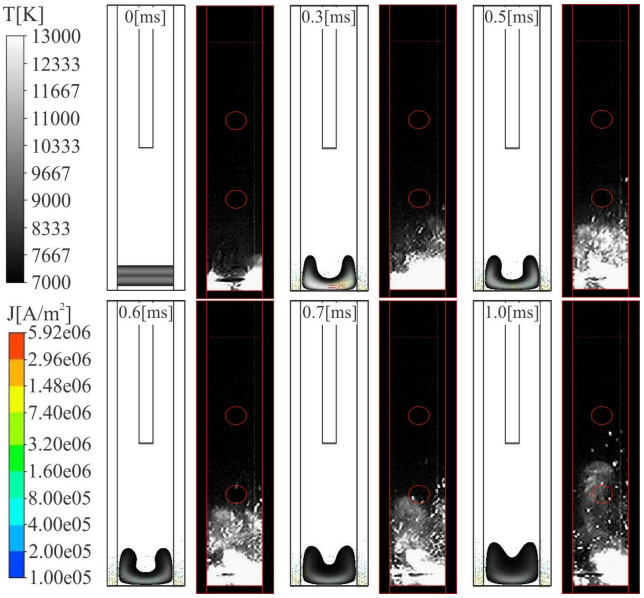

Fig. 10. Arc movement for 50A arc with 0SP and 1SP, simulation (left) and experiment (right)

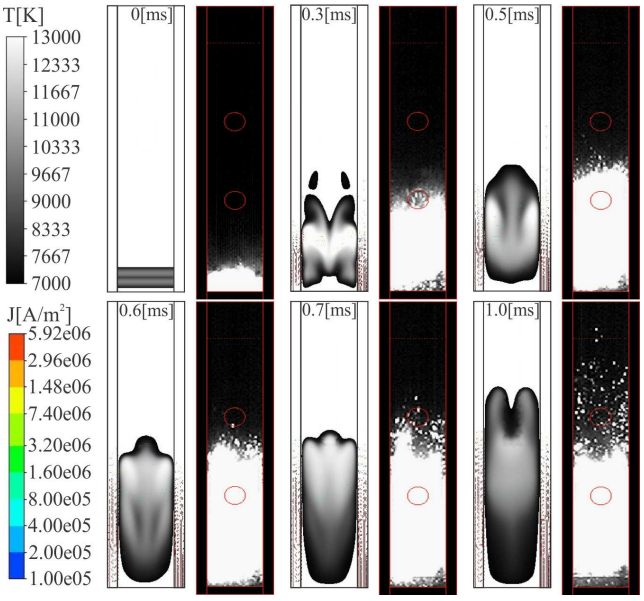

Fig. 11. Arc movement for 200A 0SP, simulation (left) and experiment (right)

This tendency together with the similar shape charts for both pressure data sets, validate that the proposed model has been correctly built.

V. Conclusions

This paper has proposed a new simulation model for analyzing the behavior of the air electric arc in LVCBs, developed in ANSYS CFX. The model reproduces a simplified chamber with four domains (air, splitter plate, cathode and anode), where the electric arc is ignited at 1mm and 10mm above the lower face of the chamber by a hot channel of 10,000K. The model is based on [16] but several improvements have been introduced, after a verification

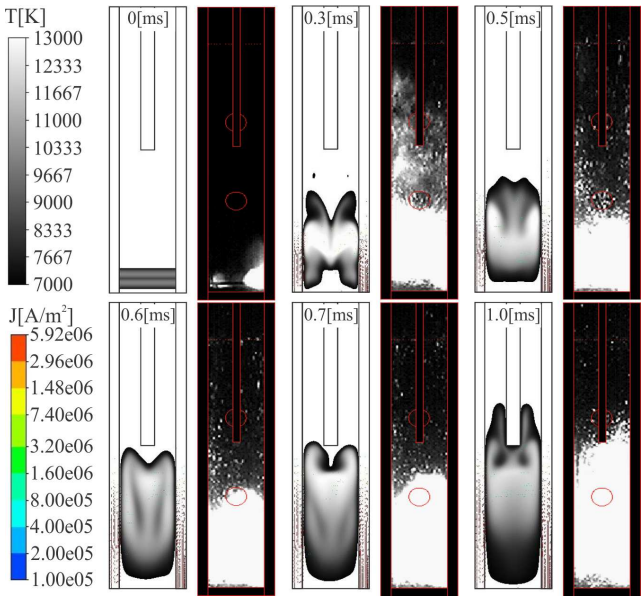

Fig. 12. Arc movement for 200A 1SP, simulation (left) and experiment (right)

process, such as: a full 3D geometry without any symmetry constraints, a fine structured and hexahedral mesh of around 1,000,000 nodes, updated thermal plasma properties and transport coefficients, P1 radiation model and the calculation of magnetic field by vector magnetic potential formulation.

Several effects have been analyzed in the new simulation model. Fist of all, the effect of the splitter plates has been analyzed, concluding that increasing the splitter plates number, the arc voltage increases, due to the lengthening of the arc and the new arc roots created. Secondly, the location for the ignition of the arc has been analyzed. The location has been tested considering the arc at 10mm and 1mm high, leading to the conclusion that low ignition location leads to slower arc movements, which represents an undesirable effect because that would lead to longer interruption time.

Finally, the input current value has been changed to analyze the effect of this parameter. It has been concluded that greater input currents lead to bigger expansion and diffusion of the arc.

All the effects tested in the simulation model have been validated through experimental testing in the laboratory. Through several experiments, the arc has been ignited at 1mm, for 0SP and 1SP at 50, 100 and 200A, recording the arc movement images, arc voltage, input current and pressure. In the experimental results, it is confirmed that a low ignition location for the arc leads to slow arcs. For 50 A, indeed, the arc does not barely move from the lower side of the arc chamber in the first six milliseconds, as it is also obtained in the simulation results. As the input current is increased in the laboratory tests, a stronger arc expansion and a faster upwards movement is observed, having the splitter plates no influence in those two phenomena. Also an elongation of the arc along the splitter plate is observed, when this is reached.

Thus, in all the cases a good correspondence between the results obtained with the simulation model and the laboratory

tests is obtained, verifying that the assumptions adopted in the proposed simulation model allow to obtain more realistic air arc behaviour results.

REFERENCES

[1] M. Anheuser, T. Beckert, and S. Kosse, "Electric arcs in switchgear - theory, numerical suimulations an experiments," in *XIXth Symposium on Physics of Switching Arc*, 2011, pp. 3–15.

[2] F. Karetta and M. Lindmayer, "Simulation of arc motion between divergent arc runners," in *Proceedings of 19th International Conference on Electric Contact Phenomena*, Tech. Univ. Braunschweig, Germany. Berlin, Germany: VDE-Verlag, 14-17 Sept. 1998 1998, pp. 361–367.

[3] M. Lindmayer and M. Springstubbe, "Three-dimensional-simulation of arc motion between arc runners including the influence of ferromagnetic material," *Components and Packaging Technologies, IEEE Transactions on*, vol. 25, no. 3, pp. 409–414, 2002.

[4] M. Lindmayer, "Simulations of switching devices based on the general transport equation," in *International Conference on Electrical Contacts Swiss Federal Institute of Technology*, 2002, pp. 01–07. [Online]. Available: http://www.elenia.tu-bs.de/forschung/veroeffentlichungen/lindmayer2002-2.pdf

[5] M. Lindmayer, E. Marzahn, A. Mutzke, and M. Springstubbe, "Low-voltage switching arcs: Experiments and modelling," in *XVth Symposium on Physics of Switching Arc*, 2003, pp. 01–16. [Online]. Available: http://htee.rz.tu-bs.de/forschung/veroeffentlichungen/LindmayerBrno2003.pdf

[6] M. Lindmayer, E. Marzahn, A. Mutzke, T. Ruther, and M. Springstubbe, "The process of arc-splitting between metal plates in low voltage arc chutes," in *50th IEEE Holm Conference on Electrical Contacts and the 22nd International Conference on Electrical Contacts*, Inst. fur Hochspannungstech. Elektrische Energieanlagen, Technische Univ. Braunschweig, Germany. Piscataway, NJ, USA: IEEE, 20-23 Sept. 2004 2004, pp. 28–34.

[7] T. Ruther, A. Mutzke, M. Lindmayer, and M. Kurrat, "The formation of arc roots on a metallic splitter plate in low-voltage arc chambers," in *23rd International Conference on Electrical Contacs*, 2006, pp. 01–06. [Online]. Available: http://www.elenia.tu-bs.de/forschung/veroeffentlichungen/ICEC2006Japan_Homepage.pdf

[8] M. Lindmayer, E. Marzahn, A. Mutzke, T. Ruther, and M. Springstubbe, "The process of arc splitting between metal plates in low voltage arc chutes," *IEEE Transactions on Components and Packaging Technologies*, vol. 29, no. 2, pp. 310–317, 2006.

[9] A. Mutzke, T. Ruther, M. Kurrat, and M. Lindmayer, "Simulation of the arc splitting proccess at a spitter plate," in *XVIIth Symposium on Physics of Switching Arc*, 10-13-IX-200 2007, pp. 01–04. [Online]. Available: http://www.htee.tu-bs.de/forschung/veroeffentlichungen/Brno2007_Homepage_mutzke.pdf

[10] A. Mutzke, T. Ruther, M. Lindmayer, and M. Kurrat, "Arc behavior in low-voltage arc chambers," in *24th International Conference on Electrical Contacts*, 2008, pp. 01–06. [Online]. Available: http://www.htee.tu-bs.de/forschung/veroeffentlichungen/Mutzke_EPJAP2008_TUBS_2009.pdf

[11] L. Xingwen and et al., "Simulation of the effects of several factors on arc plasma behavior in low voltage circuit breaker," *Plasma Science and Technology*, vol. 7, no. 5, pp. 3069–3072, 2005.

[12] L. Xingwen, C. Degui, D. Ruicheng, and G. Yingsan, "Study of the influence of arc ignition position on arc motion in low-voltage circuit breaker," *IEEE Transactions on Plasma Science*, vol. 35, no. 2, pp. 491–498, 2007.

[13] L. Xingwen, G. Chen, Y. Wu, and R. Dai, "A comparison of the effects of different mixture plasma properties on arc motion," *Journal of Physics D: Applied Physics*, vol. 40, no. 22, pp. 6982–6988, 2007. [Online]. Available: http://stacks.iop.org/0022-3727/40/i=22/a=019

[14] Y. Wu, M. Rong, Z. Sun, X. Wang, F. Yang, and X. Li, "Numerical analysis of arc plasma behaviour during contact opening process in low-voltage switching device," *Journal of Physics D (Applied Physics)*, vol. 40, no. 3, pp. 795–802, 2007.

[15] L. Xingwen, L. Rui, S. Hao, K. Tusongjiang, and C. Degui, "Ferromagnetic material effects on air arc behavior," *Plasma Science, IEEE Transactions on*, vol. 37, no. 3, pp. 463–469, 2009.

[16] M. Lohse, A. Spille-Kohoff, M. Schnick, and U. Fussel, "Implementation of lindmayer sheath model for arc simulation using ansys cfx," CFX Berlin Software GmbH; TU Dresden, Germany 2009.

[17] M. Anheuser and C. Luders, "Numerical arc simulations for low voltage circuit breakers," in *XVIIIth Symposium on Physics of Switching Arc*, 2009, pp. 1–11.

[18] C. Fievet, M. Barrault, P. Chevrier, and P. Petit, "Experimental and numerical studies of arc restrikes in low-voltage circuit breakers," *IEEE Transactions on Plasma Science*, vol. 25, no. 5, pp. 954–960, 1997.

[19] J. Wild, J. Y. Battandier, and C. Fievet, "Magneto hydrodynamic simulation coupled with network in low voltage circuit breakers," in *International Conference on Power System Technology*, vol. 2, 2004, pp. 1954–1959.

[20] A. Gleizes, Y. Cressault, and P. Teulet, "Mixing rules for thermal plasma properties in mixtures of argon, air and metallic vapours," *Plasma Sources Science and Technology*, vol. 19, no. 5, pp. 055 013–055 026, 2010. [Online]. Available: http://stacks.iop.org/0963-0252/19/i=5/a=055013

[21] F. Reichert, C. Rumpler, and F. Berger, "Application of different radiation models in the simulation of air plasma flows," in *17th International Conference on Gas Discharges and Their Applications*, 2008, pp. 141–144.

[22] A. Gleizes, J. J. Gonzalez, and P. Freton, "Thermal plasma modelling," pp. 153–183, 2005. [Online]. Available: http://stacks.iop.org/0022-3727/38/i=9/a=R01

[23] Y. Naghizadeh-Kashani, Y. Cressault, and A. Gleizes, "Net emission coefficient of air thermal plasmas," *Journal of Physics D: Applied Physics*, vol. 35, pp. 2925–2934, 2002. [Online]. Available: http://iopscience.iop.org/0022-3727/35/22/306/pdf/0022-3727_35_22_306.pdf

[24] V. Aubrecht and M. Bartlova, "Radiation transfer in thermal plasmas of air, n2 and co2," in *17th International Conference on Gas Discharges and Their Applications*, 2008, pp. 393–396.

[25] F. Reichert, "Private comunication," Technical University of Ilmenau 2011.

[26] B. Barbu, A. Iturregi, F. Berger, and E. Torres, "Analysis of spatial discretization for electric arc simulations," in *Optimization of Electrical and Electronic Equipment (OPTIM), 2012 13th International Conference on*, 2012, pp. 61–66.

[27] ——, "Numerical analysis of the electric arc simulation using ansys cfx," in *Electrical Contacts (ICEC 2012), 26th International Conference on*, 2012, pp. 311–316.

[28] P. J. Roache, *Verification and Validation in Computational Science and Engineering*. Ed: New Mexico, USA: Hermosa publishers, 1998.

[29] ——, "Quantification of uncertainty in computational fluid dynamics," *Annual Review of Fluid Mechanics*, vol. 29, no. 1, pp. 123–160, 1997.

[30] I. ANSYS, *ANSYS CFX Manual*, 2010.

[31] A. Iturregi, "Modelization and analysis of the electric arc in low voltage circuit breakers," PhD dissertation 2013.

Araitz Iturregi received her M.Sc. and Ph.D degrees in Electrical Engineering from the University of the Basque Country (UPV/EHU), Spain, in 2006 and 2013, where she currently works as a Lecturer. Her research activities are switching arcs, electric arc simulation and fault current limiting and protection in HVDC systems.

Bogdan Barbu received the Electrical Engineering degree from the Transilvania University of Brasov, Romania, in 2006. Currently he is working on his Ph.D at the Technical University of Ilmenau, Germany, focused on switching arc phenomenon.

Esther Torres received her M.Sc. and Ph.D. degrees in Electrical Engineering from the University of the Basque Country in 1998 and 2008, where she currently works as assistant Professor. Her research relays on switching arcs, analysis of power systems with distributed generation and flexible ac transmission systems applications.

Frank Berger received the Dipl.-Ing. (1984) and the Dr.-Ing. (1991) in Electrical Engineering from TU Dresden, Germany. Until 2003 he was with Moeller GmbH, Bonn, responsible for research on switching devices and switchgear. Since 2003 he has been a Full Professor for Electrical Apparatus and Switchgear at TU Ilmenau. His areas of research are switching arc phenomena, switchgear technologies and lightning protection.

Inmaculada Zamora received her M.Sc and PhD degrees in Electrical Engineering from the University of the Basque Country (UP/EHU) in 1989 and 1993, where she is a Full Professor since 2006 . Her research activities are Transients Simulation, HVDC, Fault Analysis and Protection Relaying.